Published in final edited form as:
Dev Dyn. 2014 August ; 243(8): 999–1010. doi:10.1002/dvdy.24146.

Transcriptionally Regulated Cell Adhesion Network Dictates Distal Tip Cell Directionality

Ming-Ching Wong, **William P. Kennedy**, and **Jean E. Schwarzbauer***
Department of Molecular Biology, Princeton University, Princeton, New Jersey

Abstract

Background—The mechanisms that govern directional changes in cell migration are poorly understood. The migratory paths of two distal tip cells (DTC) determine the U-shape of the C. elegans hermaphroditic gonad. The morphogenesis of this organ provides a model system to identify genes necessary for the DTCs to execute two stereotyped turns.

Results—Using candidate genes for RNAi knockdown in a DTC-specific strain, we identified two transcriptional regulators required for DTC turning: *cbp-1*, the CBP/p300 transcriptional coactivator homologue, and *let-607*, a CREBH transcription factor homologue. Further screening of potential target genes uncovered a network of integrin adhesion-related genes that have roles in turning and are dependent on *cbp-1* and *let-607* for expression. These genes include *src-1*/Src kinase, *tln-1*/talin, *pat-2*/α integrin and *nmy-2*, a nonmuscle myosin heavy chain.

Conclusions—Transcriptional regulation by means of *cbp-1* and *let-607* is crucial for determining directional changes during DTC migration. These regulators coordinate a gene network that is necessary for integrin-mediated adhesion. Overall, these results suggest that directional changes in cell migration rely on the precise gene regulation of adhesion.

Keywords

cell migration; distal tip cell; *C. elegans*; hermaphrodite gonadogenesis; integrin

INTRODUCTION

Precise regulation of cell migration is crucial for the development and maintenance of organisms. The initiation and direction must be controlled to determine when and where cells migrate. Maintaining the accuracy of these controls is integral for tissue morphogenesis, as defects in regulation can result in birth defects or cancer metastasis. Cell reorientation resulting in changes in migratory direction is critical for the formation of tissues of the correct size and shape. To accomplish these directional changes, migrating cells often rely on differential gene expression to produce proteins necessary to modulate cell adhesion, polarity, or signaling. In this study, we focus on the morphogenesis of the

*Correspondence to: Department of Molecular Biology, Princeton University, Washington Road, Princeton, NJ 08544. jschwarz@princeton.edu.

Caenorhabditis elegans hermaphroditic gonad, an organ that is defined by directional changes during cell migration.

The hermaphrodite gonad is a bi-lobed organ in which each lobe has a distinct U-shape. This shape is dictated by the migratory path of the distal tip cell (DTC), a cell that resides at the tip of the gonad arm (Wong and Schwarzbauer, 2012). Gonad morphogenesis and DTC migration are postembryonic processes (Kimble and Hirsh, 1979). Migration begins at the second larval (L2) stage (Fig. 1A) when DTCs first migrate away from the midbody, along the ventral basement membrane (BM) that overlies the body wall muscles (Hedgecock et al., 1987; Blelloch and Kimble, 1999; Nishiwaki et al., 2000). During L3, the DTCs undergo the first turn away from the ventral BM and migrate dorsally on the hypodermal BM. Once cells reach the dorsal BM, they execute a second turn back toward the midbody and proceed to migrate on the dorsal body wall muscle BM in L4 (Nishiwaki, 1999). By young adulthood, DTC migration halts at the midbody, resulting in DTCs that reside opposite from the vulva (Fig. 1A) (Hedgecock et al., 1987; Wong and Schwarzbauer, 2012).

Transcriptional regulation is important for multiple facets of DTC migration, including DTC turning (Su et al., 2000; Meighan and Schwarzbauer, 2007). For example, the DTC turn away from the ventral BM is dependent on the transcriptional activation of a netrin receptor gene *unc-5* (Su et al., 2000) and on the *blmp-1* transcriptional repressor that is required for heterochronic gene expression upstream of *unc-5* (Horn et al., 2014). Coordination of the two *C. elegans* integrin α subunits is also transcriptionally controlled. Before the first DTC turn, VAB-3, a Pax6 transcription factor, activates *pat-2* expression and subsequently represses the expression of *ina-1*, the other integrin α subunit (Meighan and Schwarzbauer, 2007). These studies suggest that transcriptional regulation is an important mode for orchestrating directional changes in cell migration.

Several genes involved in cell adhesion have been implicated in mediating the second dorsal DTC turn toward the midbody. *src-1* is the *C. elegans* homologue of the proto-oncogene Src and encodes a nonreceptor tyrosine kinase (Bei et al., 2002; Hirose et al., 2003; Itoh et al., 2005). *tln-1* encodes the ortholog for talin, a protein important for activating integrins and linking these receptors to the actin cytoskeleton (Moulder et al., 1996; Cram et al., 2003). *mig-38*, a gene with no known homologs, encodes a regulator of integrin function (Martynovsky et al., 2012). While these genes are linked by their roles downstream of integrins, the mechanism that regulates their expression remains unclear.

To gain a better understanding of how gene expression regulation coordinates DTC turning to the midbody, we conducted a candidate screen to identify transcriptional regulators required for this directional change. We identified two genes, *cbp-1* and *let-607*, and identified several of their target genes that are necessary for DTC turning. We propose a model in which the transcriptional regulators, *cbp-1* and *let-607*, coordinate the expression of an integrin-based gene network necessary for DTCs to turn back toward the midbody.

RESULTS

Transcriptional Regulators, *cbp-1* and *let-607*, Control DTC Turning

DTC-specific RNAi candidate screens were conducted to identify genes that both act cell autonomously in the DTC and are required for the DTCs to turn back toward the midbody of the hermaphrodite. DTC-specific RNAi knockdown was achieved through the use of the JK4143 strain. This strain carries a mutation in the *rde-1* gene, rendering these animals resistant to RNAi treatment, and transgenic expression of *lag-2p::rde-1* restores RNAi activity to the DTCs, but not the majority of other tissues (Martynovsky et al., 2012). Using a feeding protocol to administer RNAi treatment beginning at hatching, JK4143 nematodes were grown on bacterial strains carrying sequences of interest, through all larval stages into adulthood, and screened at the young adult stage (Cram et al., 2006). As a negative control, bacteria carrying an empty RNAi plasmid (pPD139.36/L4440) were used. This control treatment resulted in a majority of gonad arms with a wild-type phenotype (96.7%, n = 428), in which DTCs first migrated away from the midbody, then turned to migrate toward the dorsal muscles. Upon reaching the dorsal side, the DTCs turned again to migrate back toward the midbody, resulting in two stereotypic U-shaped gonadal lobes (Fig. 1A,B,E).

Candidate genes encoding transcriptional regulators that have been previously linked to DTC migration were chosen from two sources (Table 1): genes identified in a genome-wide screen (Cram et al., 2006) and lethal genes that affect DTC migration in JK4143 (Slone et al., 2011). Of the 10 transcriptional regulator genes screened, the RNAi knockdown of two genes, *cbp-1* and *let-607*, caused DTC turning defects in JK4143 animals (Fig. 1C–E). Turning defects included both the “no turn” and the “wrong turn on dorsal” phenotypes. “No turn” describes DTCs that have migrated past the turning point but have not reoriented away from the ventral BM (Fig. 1C). DTCs that have undergone the first reorientation away from the ventral BM, but did not execute the second turn on the dorsal side toward the midbody are characterized as “wrong turn” (Fig. 1D). In both cases, DTCs fail to turn back toward the midbody and result in gonad arms that extend into the head or tail of the animal. DTC-specific knockdown of *cbp-1* caused DTC turn defects in 74% (n = 420) of gonad arms and *let-607* RNAi resulted in 39% (n = 364) of DTCs with turn defects, as compared to control animals, which exhibited turn defects in less than 2% of gonad arms (n = 428) (Fig. 1E). All treatments also caused a small percentage (usually less than 5%) of “other” defects such as DTCs that stopped prematurely, meandered, or made extra turns. Overall, these results indicate that both *cbp-1* and *let-607* are required for DTCs to turn back toward the midbody.

cbp-1 and *let-607* Are Expressed in the DTCs

CBP-1, the *C. elegans* homologue of CBP/p300, is a transcriptional coactivator that functions both as a scaffold for recruiting transcriptional machinery and a chromatin remodeling enzyme through its histone acetyl-transferase activity (Chan and La Thangue, 2001; Holmqvist and Mannervik, 2013). Previous studies have shown that animals lacking *cbp-1* have an embryonic lethal phenotype due to its requirement in the differentiation of embryonic germ lineages (Shi and Mello, 1998; Victor et al., 2002). *let-607* is predicted to encode a basic leucine zipper (bZIP) transcription factor (Oommen and Newman, 2007; Reece-Hoyes et al., 2007; Silva et al., 2011) that is homologous to the cAMP response-

element binding protein H (CREBH), a CREB protein family member (Silva et al., 2011). In multiple RNAi screens, *let-607* was identified as a lethal gene (Fraser et al., 2000; Simmer et al., 2003; Rual et al., 2004; Sonnichsen et al., 2005).

Expression patterns were examined to confirm that these genes can act in a DTC autonomous manner. A *cbp-1p::RFP* transcriptional reporter strain with red fluorescent protein (RFP) controlled by a 5 kb fragment upstream of the *cbp-1* translational start site was analyzed. RFP expression was detected in most somatic cells, especially those that make up the alimentary system (data not shown), confirming previous expression profiles. Analysis of dissected gonads revealed that the DTCs also expressed RFP in stages L2 (Fig. 2A,A'), L3 (Fig. 2B,B'), and L4 (Fig. 2C,C') as well as in young adults (data not shown), indicating that *cbp-1* is expressed throughout DTC migration.

The UL1895 strain, which carries a transgene containing ~2 kb upstream of the *let-607* translational start site fused to green fluorescent protein (GFP), has previously been reported to show expression in all stages of development and in a variety of tissues (Reece-Hoyes et al., 2007). We detected GFP in the DTCs from stages L2 through late L4 (Fig. 2D–F') and through adulthood (data not shown). Taken together, the DTC expression and migration data support DTC-autonomous roles for *cbp-1* and *let-607* in the DTC turn back toward the midbody.

Identification of Genes Involved in DTC Turning

As a first step toward identifying target genes of *cbp-1* and/or *let-607*, we used RNAi and the JK4143 strain to screen more than 30 genes with known or potential roles in cell migration or adhesion for effects on DTC turning (see Table 1). Five genes from the list affected the DTC turn back toward the midbody: *src-1, tln-1, mig-38, nmy-2*, and *mlc-5*. *src-1* and *tln-1* have previously been identified as important for DTC turning (Itoh et al., 2005; Cram et al., 2006). When JK4143 animals were fed with *src-1* or *tln-1* RNAi, 51.6% (n = 634) and 36% (n = 375) of gonad arms, respectively, exhibited turning defects back to the midbody (Fig. 3A). A significant proportion of turning defects have previously been reported with *mig-38* knockdown (Martynovsky et al., 2012).

Two other genes, *nmy-2* and *mlc-5*, encode a nonmuscle myosin II heavy chain and a myosin II essential light chain, respectively (Piekny et al., 2003; Gally et al., 2009). Together, these genes have been identified as essential for embryonic morphogenesis (Gally et al., 2009), however their roles in DTC migration have not been described. DTC-specific RNAi knockdown of *nmy-2* or *mlc-5* resulted in 14.7% (n = 632) and 15.4% (n = 519) gonad arms with turn defects, respectively (Fig. 3B). *nmy-2* and *mlc-5* RNAi also caused 24.4% and 29.7% of gonad arms, respectively, to prematurely stop migrating on the dorsal BM, suggesting that nonmuscle myosins have a role in DTC motility. Taken together, these results uncover a subset of genes that have demonstrable roles in DTC turning.

Genes Regulated by *cbp-1* and *let-607*

Genes required in the DTCs for the correct turn back to the midbody might be dependent on the activity of CBP-1 and/or LET-607 for expression. To test this hypothesis, we used GFP

transcriptional reporter strains that carry a transgene with the promoter of interest driving the expression of a fluorescent protein (Table 2). Upon hatching, reporter strain animals were subjected to either *cbp-1* or *let-607* RNAi treatments until analysis. Gonadal dissections were performed to directly assess the level of reporter gene expression in the DTCs and compared with DTCs from control RNAi-treated animals.

Only 18.5% of DTCs from *src-1p::GFP* nematodes treated with *cbp-1* RNAi were GFP-positive in contrast to control RNAi treatment where the majority of DTCs expressed GFP (87.6%). *let-607* RNAi knockdown caused a similar effect, resulting in most DTCs to be void of GFP (23.1%; Fig. 4A; Table 2). A similar result was observed in *tln-1p::GFP* reporter animals. Compared with 92.5% GFP-positive *tln-1p::GFP* DTCs with control RNAi treatment, treatment with *cbp-1* RNAi caused a complete loss of GFP expression in DTCs (0% positive) and only 4.4% positive DTCs with *let-607* RNAi (Fig. 4B; Table 2). Therefore, both *src-1* and *tln-1* expression in DTCs depends on *cbp-1* and *let-607*.

The expression of *nmy-2p::GFP* relied specifically on *cbp-1*. In control treated animals, 71% of DTCs expressed GFP, but upon *cbp-1* RNAi, only 39.5% of DTC expressed GFP. By contrast, *let-607* RNAi treatment resulted in 68.1% of DTCs with GFP expression, which is similar to the control treated animals (Fig. 4C; Table 2). RNAi treatments of the translational fusion reporter strain, NMY-2::GFP also reflect this *cbp-1*-specific response (Fig. 4D; Table 2). Therefore, *nmy-2* expression is affected by *cbp-1*, but not by *let-607*. We also analyzed the transcriptional reporter strain *mlc-5p::GFP*, but the GFP expression in DTCs was very low and this strain was not amenable to this analysis. Two other candidate genes showed no DTC turning defect but their expression was affected by RNAi treatments. *UNC-112::GFP* and *unc-97p::GFP* were sensitive to levels of *cbp-1* or *let-607* (Table 2). These genes may have redundant or nonessential roles in DTC turning.

Unlike *src-1*, *tln-1*, and *nmy-2*, *mig-38p::GFP* expression was not affected by knockdown of *cbp-1* or *let-607* (Table 2). Genes that are important for initiation of DTC migration, such as basic helix-loop-helix transcription factor *mig-24* (Tamai and Nishiwaki, 2007) and the extracellular matrix gene *mig-6* (Kawano et al., 2009) were also unaffected by *cbp-1* and *let-607* RNAi treatments (Table 2). In addition, RNAi knockdown of *cbp-1* or *let-607* itself in the *let-607p::GFP* strain did not affect GFP expression in the DTCs (Table 2), indicating that DTC expression of *let-607* is not regulated by *cbp-1* or *let-607*. In general, these data reveal a subset of genes that is dependent on *cbp-1* and *let-607* for expression and also required for DTC turning.

Of the *cbp-1* and *let-607* target genes, RNAi knockdown of *src-1* or *tln-1* results in a high level of turn defects. Therefore, we wanted to determine whether *src-1* and *tln-1* were the main effectors of DTC turning in this transcriptional network. To test this, we compared the percentage of turn defects in *src-1* + control RNAi (32.3%) or *tln-1* + control RNAi (24.0%) treatment to double *src-1* + *tln-1* RNAi knockdown in JK4143 animals. This double RNAi treatment resulted in a significant increase in gonad arms with turning defects (49.8%) (Fig. 5). This percentage approaches that observed in animals treated for *cbp-1* + control RNAi, in which 60.9% of gonad arms display turning defects (Fig. 5). However, the two percentages are statistically different. This discrepancy may be due to incomplete *src-1* or *tln-1* RNAi

knockdown, because reduced efficacy of knockdown is commonly observed when diluted bacteria are used for double RNAi. This result may also suggest that there are other *cbp-1* target genes that are needed for DTCs to turn back toward the midbody.

Loss of *cbp-1*, *let-607*, or *tln-1* reduces PAT-2/α Integrin Levels in DTCs

Both *src-1* and *tln-1* genes encode proteins that have critical roles in integrin-mediated adhesion (Huveneers and Danen, 2009; Calderwood et al., 2013). Integrins *α/pat-2*, *α/ina-1*, and *β/pat-3* are expressed in the DTCs during turning. Therefore, we tested transcriptional and translational reporter strains for these integrins for their dependence on *cbp-1* and *let-607*.

In the DTCs of *pat-2p::GFP* animals, *cbp-1* RNAi caused a significant loss of GFP (4.2%). A similar effect was observed in animals treated with *let-607* RNAi (10.3%) (Fig. 6A; Table 2) compared with the majority of control *pat-2p::GFP* DTCs that expressed GFP (97.9%). In contrast, DTC *ina-1* expression was not dependent on *cbp-1* or *let-607* because 91.7% or 91.6%, respectively, of DTCs in RNAi-treated *ina-1p::RFP* animals were RFP-positive (Fig. 6B; Table 2). This result shows that only *pat-2*, the integrin that is up-regulated at the turn, is affected by knockdown of *cbp-1* or *let-607*.

Expression of *pat-2* is directly activated by VAB-3 (Meighan and Schwarzbauer, 2007). All DTCs from the *vab-3p::GFP* reporter strain expressed GFP (100%). Upon *cbp-1* RNAi treatment, all DTCs lost GFP expression. A similar effect was observed in *let-607* RNAi-treated *vab-3p::GFP* animals, in which the majority of DTCs lost GFP expression (11.4%; Fig. 6C; Table 2). Therefore, *cbp-1* and *let-607* are required for DTC-specific *vab-3* expression suggesting that *pat-2* expression is indirectly regulated by *cbp-1* and *let-607* by means of *vab-3*.

Analyses of the effects of *cbp-1* and *let-607* knockdown on integrin protein levels using translational reporter strains gave similar results. No PAT-2::GFP was detected in DTCs of animals treated with *cbp-1* (0% positive) or *let-607* RNAi (0% positive) as compared to control DTCs (94.1% positive) (Fig. 6D, Table 2). By contrast, INA-1::GFP in DTCs was unaffected by *cbp-1* or *let-607* RNAi (98% and 96% positive, respectively) as compared to control DTCs (100% positive) (Fig. 6E; Table 2). PAT-3/β integrin subunit protein levels were also insensitive to *cbp-1* or *let-607* RNAi (Fig. 6F; Table 2).

Because TLN-1 binds to integrin cytoplasmic tails and both *tln-1* and *pat-2* are regulated by *cbp-1* and *let-607*, we analyzed the effect of TLN-1 knockdown on PAT-2::GFP levels. Of interest, *tln-1* RNAi resulted in a reduction of PAT-2::GFP, with only 39.5% of DTCs expressing GFP (Fig. 6D; Table 2). This effect is specific to PAT-2 protein, as *tln-1* RNAi treatment of the *pat-2p::GFP* transcriptional fusion had no effect on DTC GFP (Table 2). The proportion of GFP-positive DTCs was also unchanged in *INA-1::GFP* and *PAT-3::GFP* strains treated with *tln-1* RNAi (Fig. 6E,F; Table 2). *src-1* RNAi had no effect on either PAT-2::GFP or INA-1::GFP (data not shown). Together, these results suggest that in addition to *cbp-1* and *let-607*-mediated transcriptional regulation of *tln-1* and *pat-2* during DTC turning, TLN-1 protein levels may also impact the stability of PAT-2 integrins.

DISCUSSION

Analysis of DTC motility and directionality during development of the *C. elegans* hermaphroditic gonad allows discovery of genes and mechanisms that regulate tissue morphogenesis. Using this model, we identified two transcriptional activators that are required for the DTCs to change direction during cell migration. The transcriptional coactivator, CBP-1, and the transcription factor, LET-607, orchestrate the expression of a cohort of integrin/adhesion-related genes that are crucial for the DTC to turn back toward the midbody. This gene network includes genes encoding the integrin *pat-2*, the transcription factor *vab-3* that activates *pat-2* expression, and the integrin and cytoskeletal-associated proteins *src-1*, *tln-1*, and *unc-97* (Fig. 7A). Two other genes, *nmy-2* and *unc-112*, depend on *cbp-1* but not *let-607*. The effects of this gene network extend to protein levels in that PAT-2::GFP levels were significantly reduced in the absence of TLN-1. We propose that these transcriptional regulators and their target genes form an adhesion gene network that coordinates changes in DTC direction to turn back toward the midbody.

Our candidate screen included a variety of transcriptional regulators, including basal transcription components, transcriptional coactivators, and transcription factors. It is notable that *cbp-1* and *let-607* are the only transcriptional regulators whose knockdown generated overt DTC turning defects. Because both *cbp-1* and *let-607* are required for embryonic and larval viability, respectively, our posthatching, tissue-specific approach was able to bypass these early requirements to uncover the role of these genes in DTC migration. Our approach also tested for the requirement of genes specifically in the DTCs, which selected against genes that affect DTC migration through potential effects on body wall muscle or hypodermal BM composition, the scaffolds on which DTCs migrate.

Vertebrate CBP was initially identified as a CREB-binding protein (Chan and La Thangue, 2001; Holmqvist and Mannervik, 2013). LET-607 is a CREB-family transcription factor (Silva et al., 2011). Because both are required for DTC turning, it seems likely that they interact to co-regulate gene expression, although no interaction data are reported on Wormbase linking these two genes. It is also possible that CBP-1 can interact with other CREB homologs in *C. elegans*. Despite broad expression of the CREB homolog *crh-2*, RNAi knockdown in DTCs did not result in a migration or gonad morphology phenotype (Table 1).

As a CREB-family transcription factor, LET-607 would be predicted to bind CREB-response element (CRE) DNA consensus sites to regulate transcription (Zhang et al., 2005). Promoters of genes that are dependent on *cbp-1* and *let-607* were analyzed for CRE sites. We found that the *tln-1* promoter contains a full CRE site (TGACGTCA) within 600 bp of the transcription start site. Also, both *tln-1* and *src-1* promoter regions have half CRE sites (TGACG/CGTCA) within 200 bp of the transcriptional start site (W.P.K. and M.C.W., unpublished observations); half CRE sites have also been shown to be functional (Zhang et al., 2005). Further analysis of these sites would reveal the dependence of *tln-1* expression on CREB family proteins.

CBP-1 is not predicted to directly bind DNA, but binds to transcription factors to exert regulatory influence on transcription. Vertebrate CBP has been shown to interact with a variety of transcription factors, including CREB, Smads, FOXO, and MYC (Iwamoto et al., 2002; Vervoorts et al., 2003; van der Heide and Smidt, 2005; Holmqvist and Mannervik, 2013). Based on this evidence, it is likely that CBP-1 influences a larger set of target genes compared with LET-607. Our data support this, as CBP-1 is required for the same subset of genes as LET-607, as well as *nmy-2* and *unc-112*.

The identification of *nmy-2* as a gene necessary for DTC turning reveals a role for this force-generating protein in directional changes in migration. Previous work has shown that when DTCs migrate dorsally on the hypodermal BM, the DTC forms a single lamellipodium in the direction of migration and then retracts its trailing edge as it shifts its migration to the dorsal BM (Kim et al., 2011). This mode of migration may depend on the contractile activity of NMY-2 and could be necessary for the DTC to transition from the hypodermal BM to the dorsal BM.

Previous work has revealed that the two α integrins in *C. elegans* have distinct roles in DTC migration. INA-1, which is expressed in DTCs at the initiation of migration, is important for migration, whereas PAT-2, which is activated by VAB-3 and up-regulated before DTC turning, is important for DTC pathfinding and directionality (Meighan and Schwarzbauer, 2007). Our findings correlate with these data; *pat-2* and *vab-3*, but not *ina-1*, rely on CBP-1 and LET-607. Furthermore, the different roles of PAT-2 and INA-1 integrins might also require selective use of focal adhesion proteins. For example, over-expression of a SRC-1::RFP transgene in the DTCs caused premature stopping on the ventral side in L2 (M.C.W., unpublished observations), which may indicate that excess SRC-1 can affect INA-1/PAT-3 activity, possibly to increase adhesion. On the other hand, reduction in *src-1* expression by RNAi treatments or mutation (this study; Lee et al., 2005; Itoh et al., 2005) causes DTC turning defects but not other DTC migratory defects. Based on this phenotype, *src-1* expression in L3 may be involved primarily in PAT-2/PAT-3 integrin signaling (Fig. 7B,C).

We propose a model that incorporates the temporal changes in gene expression with effects on motility and turning. At initiation of migration, DTCs express INA-1/PAT-3 integrin, TLN-1, and NMY-2 (Fig. 7B). The integrin is linked to the actin cytoskeleton by means of TLN-1 and indirectly associated with NMY-2. *vab-3* expression just before the turn induces *pat-2* expression so that at the time of turning, DTCs have both INA-1/PAT-3 and PAT-2/PAT-3 integrins (Fig. 7C). Increased numbers of integrin receptors could then require increased expression of TLN-1 and NMY-2. Up-regulation of *src-1* expression would facilitate PAT-2/PAT-3 activity at the turn and, along with TLN-1, stabilize its connection to the cytoskeleton. Because PAT-2/PAT-3 is highly expressed in body wall muscle, where the ability to withstand force and tension is critical, it is possible that PAT-2/PAT-3 and associated proteins such as SRC-1 and TLN-1 are required to strengthen cell adhesion as the DTCs maneuver the turn. During turning, however, it is essential for the DTC to switch its adhesion to different BMs (ventral muscle to hypodermal to dorsal muscle BM). Therefore, the changes in gene expression may be critical for the precise regulation of adhesion strength and detachment necessary for DTC turning.

This integrin/adhesion-related gene network that is transcriptionally regulated by CBP-1 and LET-607 and is crucial for DTC turning may have broader implications in directional cell migration. Modulation of adhesion stability through gene expression might be an effective mode of regulation for cells to exert changes in cell migration direction. This or a related gene network may be involved in responses to chemoattractants or changes in BM composition in other developmental systems or in disease states.

EXPERIMENTAL PROCEDURES

Nematode Strains

Animals were cultured at 20°C under standard conditions (Brenner, 1974). The JE0107 *mwEx107[cbp-1p::RFP, rol-6(su1006)]* strain carries a transcriptional fusion construct made by fusing 5 kb of the sequence upstream from the *cbp-1* translational start site to the mRFP cDNA. This construct was generated using PCR fusion technique (Hobert, 2002) and injected into N2 animals. The following nematode strains were also used in this study: JK4143 [*lag-2p::GFP* (*qIs57 II*); *rde-1 (ne219) V; lag-2p::rde-1* (*qIs140*)] (Martynovsky et al., 2012); UL1894 [*let-607p::GFP* (nonintegrated)] (Reece-Hoyes et al., 2007); *psrc-1::GFP* (nonintegrated) (Hirose et al., 2003); SK4015 [*tln-1p::GFP (zdIs15)*] (Cram et al., 2006); JJ1473 [*NMY-2::GFP* (*zuIs45*)] (Nance et al., 2003); JE2121 [*pat-2p::GFP* (*jeIs2121*)] (Meighan and Schwarzbauer, 2007); NG2517 [*INA-1::GFP* (*gmIs5*)] (Baum and Garriga, 1997); JE1111 [*ina-1p::RFP* (nonintegrated)] (Meighan and Schwarzbauer, 2007); NF2168 [*mig-24p::Venus (tkIs11)*] (Tamai and Nishiwaki, 2007); JE2222 [*PAT-2::GFP* (*jeIs2222*)] (Meighan and Schwarzbauer, 2007); *PAT-3::GFP* [*pat-3(rh151); rhEx1[-pat-3::GFP]*] (Plenefisch et al., 2000); DM8008 [*UNC-112::GFP* (*raIs8*)] (Rogalski et al., 2000); BC10577 [*vab-3p::GFP* (*sEx10577*)]; BC12753 [*mig-38p::GFP* (*sIs12371*)], BC15734 [*mig-6p::GFP* (*sIs14164*)], BC11043 [*unc-97p::GFP* (*sEx11043*)]; BC14855 [*nmy-2p::GFP* (*sEx14855*)]; BC12988 [*arr-1p::GFP* (*sIs12777*)]; BC15466 [*mlc-5p::GFP* (*sEx15466*)] (McKay et al., 2003).

RNAi Treatments

RNAi treatments were administered using the feeding protocol (Fraser et al., 2000), as previously described (Wong et al., 2011; Martynovsky et al., 2012). Briefly, HT115(DE3) *E. coli* carrying the pPD129.36/L4440 plasmid with appropriate gene inserts were cultured overnight in LB ampicillin liquid culture and plated on NGM plates supplemented with 1 mM IPTG to induce dsRNA production overnight. Eggs were isolated from gravid hermaphrodites; the eggs were plated on induced bacteria, allowed to hatch, and cultured until the appropriate stage for analysis. Control RNAi animals were fed HT115 bacteria carrying the pPD129.36/L4440 plasmid with no insert. This RNAi feeding method bypasses all embryonic gene requirements and allows for the assessment of DTC migration roles for genes required during early development. All RNAi treatments presented within a graph were performed in tandem and all RNAi experiments (assaying gonad morphology and fluorescence in DTCs) represent the results of three independent experiments that were pooled to give the final percentages shown. RNAi treatment using JK4143 animals identifies DTC-autonomous effects of genes, but may reduce the strength of RNAi knockdown, resulting in less penetrant DTC phenotypes compared with phenotypes from global RNAi

knockdown (Cram et al., 2003, 2006; Lee et al., 2005). RNAi clones were obtained from Geneservice. All clones were from the Ahringer RNAi library (Fraser et al., 2000), except *deb-1* RNAi from the Vidal library (Rual et al., 2004) and *src-1* RNAi (Cram et al., 2006).

Microscopy and Gonad Dissections

Both whole-mount animals and DTCs from dissected gonads were visualized using a Nikon T-2000 microscope. In many strains, the reporter plasmids are propagated extrachromosomally; only DTCs from animals expressing the fluorescent transgene were analyzed. Images were captured using either a Hamamatsu ORIA ER-4 camera or a Q-Imaging camera (QICAM) and iVision software. Images were processed and assembled using Photoshop. Gonad dissection was performed using a 26-G needle in PBS/0.2 mM levamisole. Nematodes were decapitated and the extruded gonads were analyzed. Fluorescence levels in DTCs from control RNAi-fed animals were evaluated and compared by eye to RNAi-treated animals. Within experiments, fluorescent DTC images were captured using the same exposure time and were normalized to the control treatment DTC. Mosaicism was observed in certain strains with varied levels of GFP expression in the DTCs. Therefore, GFP levels were not quantified but instead DTCs were scored as being either GFP-positive or GFP-negative.

Gonad Morphology Phenotypes and Statistical Analysis

For the analysis of gonad morphology, whole nematodes were mounted on 2% agarose pads, and scored at the L4/young adult stage, as previously described (Wong et al., 2011). Unless otherwise stated, DTC migration phenotype percentages were presented in graphs grouped into three categories: wild-type, turn defects, other. Turn defects include gonad arms that exhibit the “no turn” or “wrong turn” phenotypes. The “other” phenotypic category includes gonad arms in which DTC migration prematurely stopped, or gonad arms with pathfinding defects, in which DTCs have deviated from the wild-type path by meandering or making supernumerary turns. In general, each of these “other” phenotypes consisted of less than 5% of total gonad arms scored, unless otherwise noted.

Statistical analysis of gonad phenotypes was performed using the chi-squared test of independence (McDonald, 2009). Comparisons were made between two different RNAi treatments, as noted. Either all phenotypic categories (wild-type/turning defects/other phenotypes) or specific phenotypic categories, such as turning defects, (turning defects/nonturning defects, which includes wild-type and other phenotypes) were compared, as indicated. Error bars in graphs represent 95% confidence intervals for proportions (Bewick et al., 2004).

ACKNOWLEDGMENTS

We thank Kiyoji Nishiwaki, Donald Moerman, Bunsho Ito, and Ian Hope for nematode strains, and Erin Cram for the *src-1* RNAi construct. Some strains were provided by the CGC, which is funded by NIH Office of Research Infrastructure Programs. J.E.S. was funded by the NIH and by the Cell Migration Consortium GLUE grant. M.C.W. was a postdoctoral fellow of the New Jersey Commission on Cancer Research.

Grant sponsor: NIH; Grant number: R01GM059383; Grant number: U54 GM064346; Grant sponsor: New Jersey Commission for Cancer Research; Grant number: 10-2409-CCR-EO.

REFERENCES

Baum PD, Garriga G. Neuronal migrations and axon fasciculation are disrupted in ina-1 integrin mutants. Neuron. 1997; 19:51–62. [PubMed: 9247263]

Bei Y, Hogan J, Berkowitz LA, Soto M, Rocheleau CE, Pang KM, Collins J, Mello CC. SRC-1 and Wnt signaling act together to specify endoderm and to control cleavage orientation in early C. elegans embryos. Dev Cell. 2002; 3:113–125. [PubMed: 12110172]

Bewick V, Cheek L, Ball J. Statistics review 8: qualitative data - tests of association. Crit Care. 2004; 8:46–53. [PubMed: 14975045]

Blelloch R, Kimble J. Control of organ shape by a secreted metalloprotease in the nematode Caenorhabditis elegans. Nature. 1999; 399:586–590. [PubMed: 10376599]

Brenner S. The genetics of Caenorhabditis elegans. Genetics. 1974; 77:71–94. [PubMed: 4366476]

Calderwood DA, Campbell ID, Critchley DR. Talins and kindlins: partners in integrin-mediated adhesion. Nat Rev Mol Cell Biol. 2013; 14:503–517. [PubMed: 23860236]

Chan HM, La Thangue NB. p300/CBP proteins: HATs for transcriptional bridges and scaffolds. J Cell Sci. 2001; 114:2363–2373. [PubMed: 11559745]

Cram EJ, Clark SG, Schwarzbauer JE. Talin loss-of-function uncovers roles in cell contractility and migration in C. elegans. J Cell Sci. 2003; 116:3871–3878. [PubMed: 12915588]

Cram EJ, Shang H, Schwarzbauer JE. A systematic RNA interference screen reveals a cell migration gene network in C. elegans. J Cell Sci. 2006; 119:4811–4818. [PubMed: 17090602]

Fraser AG, Kamath RS, Zipperlen P, Martinez-Campos M, Sohrmann M, Ahringer J. Functional genomic analysis of C. elegans chromosome I by systematic RNA interference. Nature. 2000; 408:325–330. [PubMed: 11099033]

Gally C, Wissler F, Zahreddine H, Quintin S, Landmann F, Labouesse M. Myosin II regulation during C. elegans embryonic elongation: LET-502/ROCK, MRCK-1 and PAK-1, three kinases with different roles. Development. 2009; 136:3109–3119. [PubMed: 19675126]

Hedgecock EM, Culotti JG, Hall DH, Stern BD. Genetics of cell and axon migrations in Caenorhabditis elegans. Development. 1987; 100:365–382. [PubMed: 3308403]

Hirose T, Koga M, Ohshima Y, Okada M. Distinct roles of the Src family kinases, SRC-1 and KIN-22, that are negatively regulated by CSK-1 in C. elegans. FEBS Lett. 2003; 534:133–138. [PubMed: 12527374]

Hobert O. PCR fusion-based approach to create reporter gene constructs for expression analysis in transgenic C. elegans. Biotechniques. 2002; 32:728–730. [PubMed: 11962590]

Holmqvist PH, Mannervik M. Genomic occupancy of the transcriptional co-activators p300 and CBP. Transcription. 2013; 4:18–23. [PubMed: 23131664]

Horn M, Geisen C, Cermak L, Becker B, Nakamura S, Klein C, Pagano M, Antebi A. DRE-1/FBXO11-dependent degradation of BLMP-1/BLIMP-1 governs C. elegans developmental timing and maturation. Dev Cell. 2014; 28:697–710. [PubMed: 24613396]

Huveneers S, Danen EH. Adhesion signaling - crosstalk between integrins, Src and Rho. J Cell Sci. 2009; 122:1059–1069. [PubMed: 19339545]

Itoh B, Hirose T, Takata N, Nishiwaki K, Koga M, Ohshima Y, Okada M. SRC-1, a non-receptor type of protein tyrosine kinase, controls the direction of cell and growth cone migration in C. elegans. Development. 2005; 132:5161–5172. [PubMed: 16251208]

Iwamoto T, Oshima K, Seng T, Feng X, Oo ML, Hamaguchi M, Matsuda S. STAT and SMAD signaling in cancer. Histol Histopathol. 2002; 17:887–895. [PubMed: 12168800]

Kawano T, Zheng H, Merz DC, Kohara Y, Tamai KK, Nishiwaki K, Culotti JG. C. elegans mig-6 encodes papilin isoforms that affect distinct aspects of DTC migration, and interacts genetically with mig-17 and collagen IV. Development. 2009; 136:1433–1442. [PubMed: 19297413]

Kim HS, Murakami R, Quintin S, Mori M, Ohkura K, Tamai KK, Labouesse M, Sakamoto H, Nishiwaki K. VAB-10 spectra-plakin acts in cell and nuclear migration in Caenorhabditis elegans. Development. 2011; 138:4013–4023. [PubMed: 21831923]

Kimble J, Hirsh D. The postembryonic cell lineages of the hermaphrodite and male gonads in Caenorhabditis elegans. Dev Biol. 1979; 70:396–417. [PubMed: 478167]

Lee J, Li W, Guan KL. SRC-1 mediates UNC-5 signaling in Caenorhabditis elegans. Mol Cell Biol. 2005; 25:6485–6495. [PubMed: 16024786]

Martynovsky M, Wong MC, Byrd DT, Kimble J, Schwarzbauer JE. mig-38, a novel gene that regulates distal tip cell turning during gonadogenesis in C. elegans hermaphrodites. Dev Biol. 2012; 368:404–414. [PubMed: 22732572]

McDonald, JH. Handbook of biological statistics. Sparky House Publishing; Baltimore, MD: 2009. Chi-square test of independence; p. 57-63.

McKay SJ, Johnsen R, Khattra J, Asano J, Baillie DL, Chan S, Dube N, Fang L, Goszczynski B, Ha E, Halfnight E, Hollebakken R, Huang P, Hung K, Jensen V, Jones SJ, Kai H, Li D, Mah A, Marra M, McGhee J, Newbury R, Pouzyrev A, Riddle DL, Sonnhammer E, Tian H, Tu D, Tyson JR, Vatcher G, Warner A, Wong K, Zhao Z, Moerman DG. Gene expression profiling of cells, tissues, and developmental stages of the nematode C. elegans. Cold Spring Harb Symp Quant Biol. 2003; 68:159–169. [PubMed: 15338614]

Meighan CM, Schwarzbauer JE. Control of C. elegans hermaphrodite gonad size and shape by vab-3/Pax6-mediated regulation of integrin receptors. Genes Dev. 2007; 21:1615–1620. [PubMed: 17606640]

Moulder GL, Huang MM, Waterston RH, Barstead RJ. Talin requires beta-integrin, but not vinculin, for its assembly into focal adhesion-like structures in the nematode Caenorhabditis elegans. Mol Biol Cell. 1996; 7:1181–1193. [PubMed: 8856663]

Nance J, Munro EM, Priess JR. C. elegans PAR-3 and PAR-6 are required for apicobasal asymmetries associated with cell adhesion and gastrulation. Development. 2003; 130:5339–5350. [PubMed: 13129846]

Nishiwaki K. Mutations affecting symmetrical migration of distal tip cells in Caenorhabditis elegans. Genetics. 1999; 152:985–997. [PubMed: 10388818]

Nishiwaki K, Hisamoto N, Matsumoto K. A metalloprotease disintegrin that controls cell migration in Caenorhabditis elegans. Science. 2000; 288:2205–2208. [PubMed: 10864868]

Oommen KS, Newman AP. Co-regulation by Notch and Fos is required for cell fate specification of intermediate precursors during C. elegans uterine development. Development. 2007; 134:3999–4009. [PubMed: 17942488]

Piekny AJ, Johnson JL, Cham GD, Mains PE. The Caenorhabditis elegans nonmuscle myosin genes nmy-1 and nmy-2 function as redundant components of the let-502/Rho-binding kinase and mel-11/myosin phosphatase pathway during embryonic morphogenesis. Development. 2003; 130:5695–5704. [PubMed: 14522875]

Plenefisch JD, Zhu X, Hedgecock EM. Fragile skeletal muscle attachments in dystrophic mutants of Caenorhabditis elegans: isolation and characterization of the mua genes. Development. 2000; 127:1197–1207. [PubMed: 10683173]

Reece-Hoyes JS, Shingles J, Dupuy D, Grove CA, Walhout AJ, Vidal M, Hope IA. Insight into transcription factor gene duplication from Caenorhabditis elegans Promoterome-driven expression patterns. BMC Genomics. 2007; 8:27. [PubMed: 17244357]

Rogalski TM, Mullen GP, Gilbert MM, Williams BD, Moerman DG. The UNC-112 gene in Caenorhabditis elegans encodes a novel component of cell-matrix adhesion structures required for integrin localization in the muscle cell membrane. J Cell Biol. 2000; 150:253–264. [PubMed: 10893272]

Rual JF, Ceron J, Koreth J, Hao T, Nicot AS, Hirozane-Kishikawa T, Vandenhaute J, Orkin SH, Hill DE, van den Heuvel S, Vidal M. Toward improving Caenorhabditis elegans phenome mapping with an ORFeome-based RNAi library. Genome Res. 2004; 14:2162–2168. [PubMed: 15489339]

Shi Y, Mello C. A CBP/p300 homolog specifies multiple differentiation pathways in Caenorhabditis elegans. Genes Dev. 1998; 12:943–955. [PubMed: 9531533]

Silva MC, Fox S, Beam M, Thakkar H, Amaral MD, Morimoto RI. A genetic screening strategy identifies novel regulators of the proteostasis network. PLoS Genet. 2011; 7:e1002438. [PubMed: 22242008]

Simmer F, Moorman C, van der Linden AM, Kuijk E, van den Berghe PV, Kamath RS, Fraser AG, Ahringer J, Plasterk RH. Genome-wide RNAi of C. elegans using the hypersensitive rrf-3 strain reveals novel gene functions. PLoS Biol. 2003; 1:E12. [PubMed: 14551910]

Slone, RD.; Byrd, D.; Kimble, J.; Schwarzbauer, JE. A DTC-specific RNAi screen of lethal genes. Cell migration gateway: cell migration consortium. 2011. http://www.cellmigration.org/resource/discovery/schwarzbauer/schwarzbauer_rnai3a.cgi

Sonnichsen B, Koski LB, Walsh A, Marschall P, Neumann B, Brehm M, Alleaume AM, Artelt J, Bettencourt P, Cassin E, Hewitson M, Holz C, Khan M, Lazik S, Martin C, Nitzsche B, Ruer M, Stamford J, Winzi M, Heinkel R, Roder M, Finell J, Hantsch H, Jones SJ, Jones M, Piano F, Gunsalus KC, Oegema K, Gonczy P, Coulson A, Hyman AA, Echeverri CJ. Full-genome RNAi profiling of early embryogenesis in Caenorhabditis elegans. Nature. 2005; 434:462–469. [PubMed: 15791247]

Su M, Merz DC, Killeen MT, Zhou Y, Zheng H, Kramer JM, Hedgecock EM, Culotti JG. Regulation of the UNC-5 netrin receptor initiates the first reorientation of migrating distal tip cells in Caenorhabditis elegans. Development. 2000; 127:585–594. [PubMed: 10631179]

Tamai KK, Nishiwaki K. bHLH transcription factors regulate organ morphogenesis via activation of an ADAMTS protease in C. elegans. Dev Biol. 2007; 308:562–571. [PubMed: 17588558]

van der Heide LP, Smidt MP. Regulation of FoxO activity by CBP/p300-mediated acetylation. Trends Biochem Sci. 2005; 30:81–86. [PubMed: 15691653]

Vervoorts J, Luscher-Firzlaff JM, Rottmann S, Lilischkis R, Walsemann G, Dohmann K, Austen M, Luscher B. Stimulation of c-MYC transcriptional activity and acetylation by recruitment of the cofactor CBP. EMBO Rep. 2003; 4:484–490. [PubMed: 12776737]

Victor M, Bei Y, Gay F, Calvo D, Mello C, Shi Y. HAT activity is essential for CBP-1-dependent transcription and differentiation in Caenorhabditis elegans. EMBO Rep. 2002; 3:50–55. [PubMed: 11751575]

Wong MC, Martynovsky M, Schwarzbauer JE. Analysis of cell migration using Caenorhabditis elegans as a model system. Methods Mol Biol. 2011; 769:233–247. [PubMed: 21748680]

Wong MC, Schwarzbauer JE. Gonad morphogenesis and distal tip cell migration in the Caenorhabditis elegans hermaphrodite. Wiley Interdiscip Rev Dev Biol. 2012; 1:519–531. [PubMed: 23559979]

Zhang X, Odom DT, Koo SH, Conkright MD, Canettieri G, Best J, Chen H, Jenner R, Herbolsheimer E, Jacobsen E, Kadam S, Ecker JR, Emerson B, Hogenesch JB, Unterman T, Young RA, Montminy M. Genome-wide analysis of cAMP-response element binding protein occupancy, phosphorylation, and target gene activation in human tissues. Proc Natl Acad Sci U S A. 2005; 102:4459–4464. [PubMed: 15753290]

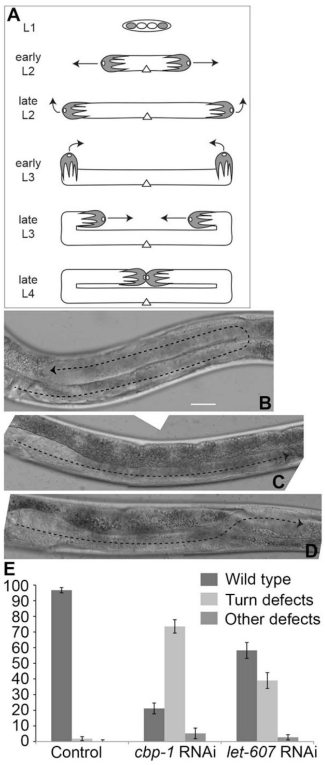

Fig. 1.

Transcriptional regulators are required for DTC turning. **A:** During hermaphroditic gonadogenesis, the two DTCs (gray cells) are born in stage L1 and migrate along mirror imaged, U-shaped paths. By late stage L4, the migratory path of the DTC is reflected by the final morphology of the gonad arm. **B–D:** Differential interference contrast (DIC) images of posterior gonad arms in the JK4143 [*rde-1 (ne219); lag-2p::rde-1*] strain treated with control RNAi (B) and *cbp-1* RNAi [“no turn” (C) and “wrong turn” (D) phenotypes shown]. This strain is sensitive to RNAi in a DTC-specific manner. Dotted arrows reflect the DTC migratory path. Scale bar = 20 μm. **E:** Graph shows the percentages of gonad morphologies observed in control (n = 428), *cbp-1* (n = 420) or *let-607* (n = 364) RNAi-treated JK4143 animals, where n is the number of observed gonad arms. Phenotypes were categorized as “wild-type” (dark gray), “turn defects” (light gray), or “other” (medium gray). The “turn defects” category includes both “no turn” and “wrong turn” phenotypes. Error bars represent 95% confidence intervals. Differences between control and *cbp-1* or *let-607* RNAi treatment groups are significant ($P < 0.001$).

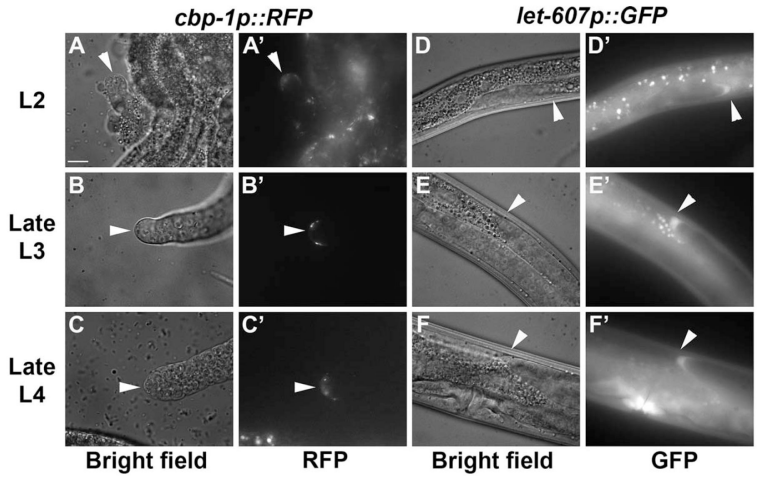

Fig. 2.

cbp-1 and *let-607* are expressed in migrating DTCs. Analysis of the reporter strains, *cbp-1p::RFP* (**A–C**') and *let-607p::GFP* (**D–F**'), reveals fluorescent protein expression in the DTCs from stage L2 (A,A',D,D') through late L4 (C,C',F,F'). DIC (A–F) and epifluorescence (A'–F') images were captured for dissected DTCs from *cbp-1p::RFP* (A–C') or whole animal mounts of *let-607p::GFP* (D–F') transcriptional fusion strains. White arrowheads indicate DTCs. Scale bar = 10 μm.

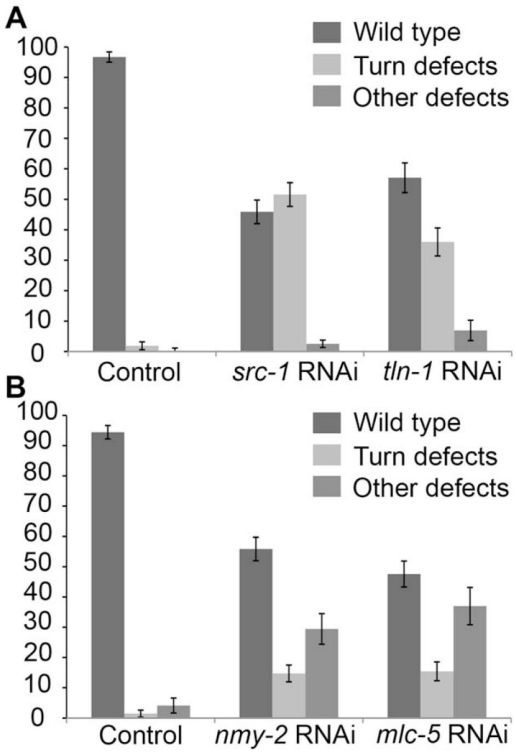

Fig. 3.

Identification of genes involved in DTC turning. Strain JK4143 fed control or gene-specific RNAi bacteria and gonad arm morphologies were categorized as indicated. The percentages of gonad morphologies are shown for (**A**) control (n = 428), *src-1* (n = 634), or *tln-1* (n = 375) RNAi treatments and (**B**) control (n = 414), *nmy-2* (n = 632), or *mlc-5* (n = 519) RNAi. All error bars represent 95% confidence intervals. Differences between control versus *src-1* or *tln-1* RNAi treatment and control versus *nmy-2* or *mlc-5* RNAi treatment groups are significant ($P < 0.001$).

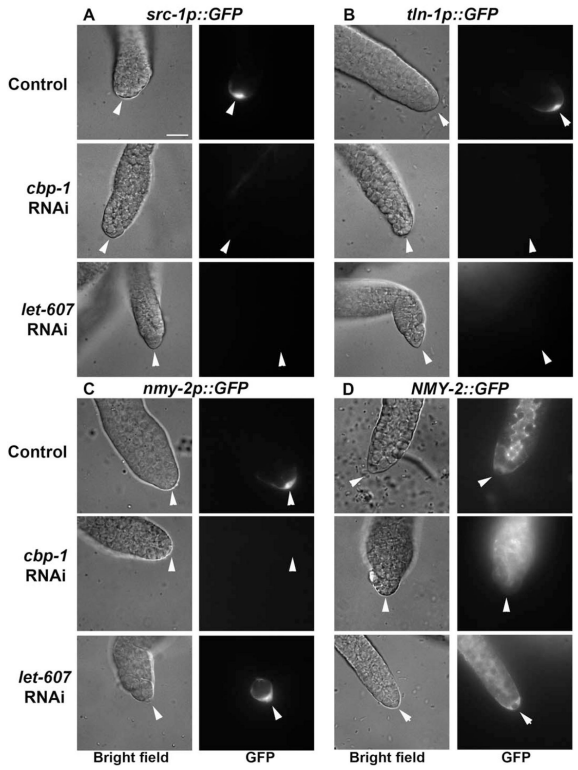

Fig. 4.

Roles for *cbp-1* and *let-607* in expression of *src-1*, *tln-1*, and *nmy-2*. Transgenic GFP reporter strains carrying transcriptional or translational fusion constructs were used to analyze the effect of *cbp-1* or *let-607* RNAi treatment on GFP expression in DTCs. Representative DIC and fluorescence images of the reporter strains *src-1p::GFP* (**A**), *tln-1p::GFP* (**B**), *nmy-2p::GFP* (**C**), and *NMY-2::GFP* (**D**) are shown. Transgenic strains were fed control, *cbp-1*, or *let-607* RNAi bacteria. All images are of dissected DTCs from adult or young adult hermaphrodites. Within an experiment, images were normalized to the control DTC. White arrowheads indicate DTCs. Scale bar = 10 μm.

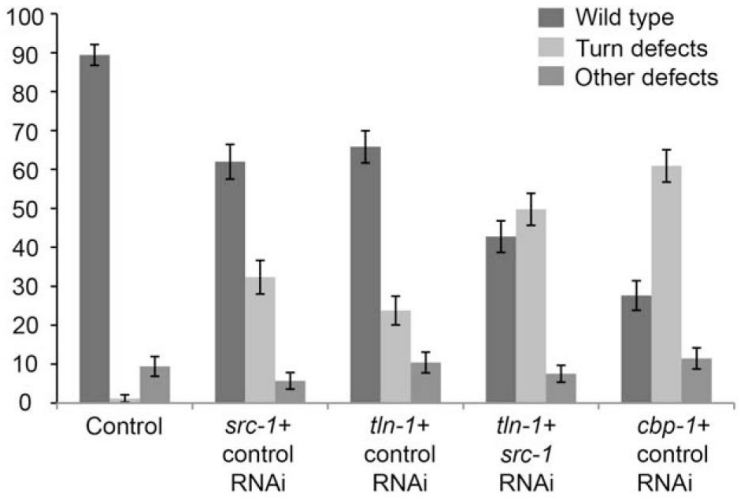

Fig. 5.

Double knockdown of *tln-1* + *src-1* and knockdown of *cbp-1* give similar levels of turn defects. Graph shows the percentages of gonad morphologies observed in JK4143 animals treated with control (n = 510), *src-1* + control (n = 455), *tln-1* + control (n = 509), *tln-1* + *src-1* (n = 571) and *cbp-1* + control (n = 532) RNAi. Phenotypes were categorized as indicated. The *src-1* + control and *tln-1* + control groups are significantly different from *src-1* + *tln-1* ($P < 0.001$). *tln-1* + *src-1* data are statistically different from *cbp-1* + control ($P < 0.001$). Error bars represent 95% confidence intervals.

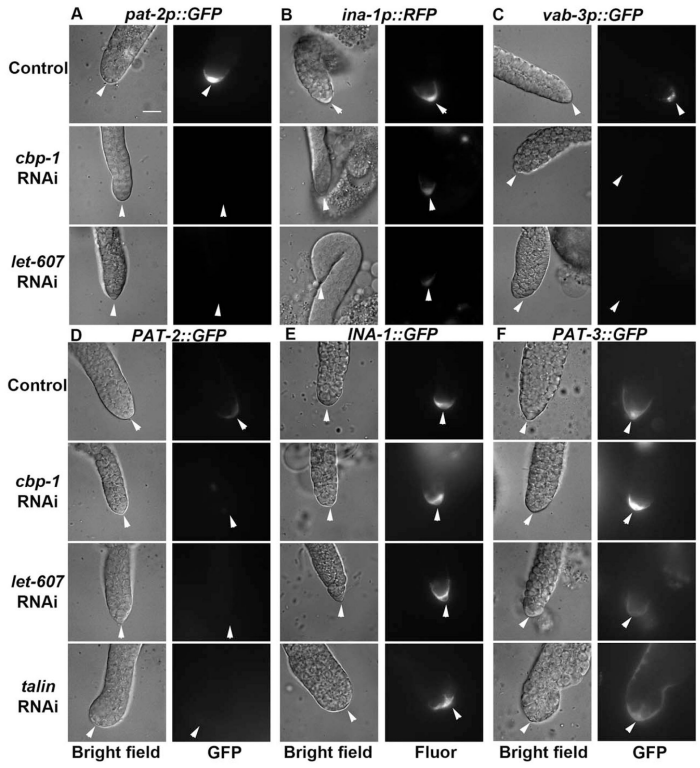

Fig. 6.

Effects of cbp-1 or let-607 RNAi on integrin expression. Transcriptional and translational fusion reporter strains, *pat-2p::GFP* (**A**), *ina-1p::RFP* (**B**), *vab-3p::GFP* (**C**), *PAT-2::GFP* (**D**), *INA-1::GFP* (**E**), and *PAT-3::GFP* (**F**) were used to determine the effect of *cbp-1*, *let-607* or *tln-1* knockdown on expression in DTCs. DIC and fluorescence images of dissected DTCs from animals treated with control, *cbp-1*, *let-607*, or *tln-1* RNAi are shown. Within an experiment, images were normalized to the control DTC. All images are of dissected DTCs from young adult hermaphrodites, except for *ina-1p::RFP* (B) and *INA-1::GFP* (E), which show DTCs from late L3/early L4 animals. White arrowheads indicate DTCs. Scale bar = 10 μm.

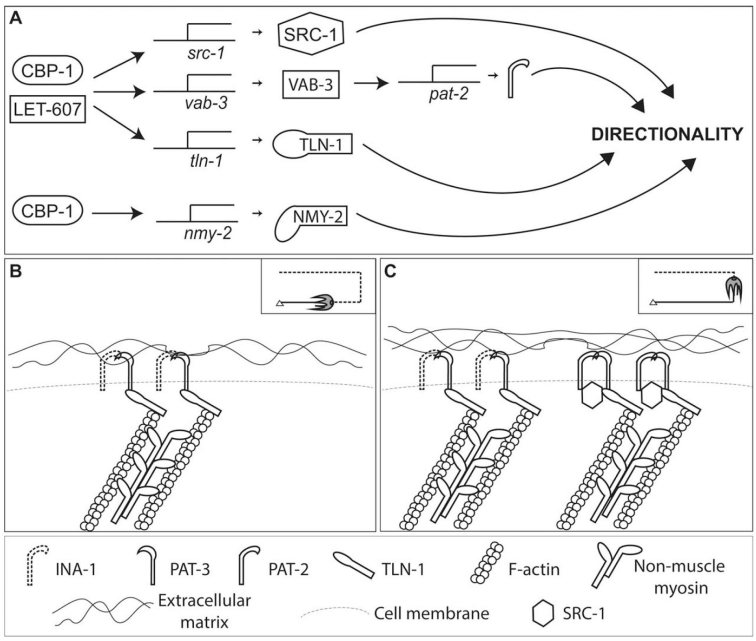

Fig. 7.

CBP-1 and LET-607 orchestrate expression of an integrin/adhesion gene network necessary for DTC directionality. **A:** Schematic summarizing the gene network required for DTC turning. CBP-1 and LET-607 are required for expression of *src-1*, *vab-3*, and *tln-1*. Independently of LET-607, CBP-1 is required for *nmy-2* expression. VAB-3 expression is initiated at the onset of DTC turning, and regulates the expression of the α integrin, *pat-2*. These genes are important for DTC directionality. **B:** During migration on the ventral BM, the DTC expresses INA-1/PAT-3 integrin, the integrin-actin cytoskeletal linker protein TLN-1, and the acto-myosin contractile protein NMY-2. **C:** During turning, the DTC expresses both INA-1/PAT-3 and PAT-2/PAT-3 integrins and TLN-1 expression is up-regulated. SRC-1 is required for turning and its primary role may be through association with PAT-2/PAT-3 adhesions. Insets in B and C are schematics showing the migration progress of a posterior DTC cell. See text for a detailed description of the model.

TABLE 1

Candidate Genes Screened for DTC Turning and Expression[a]

Gene name	Sequence	Protein description
Transcriptional regulators		
sup-37	C01B7.1	C2H2 zinc finger transcription factor
tlf-1	F39H11.2	TATA binding protein (TBP)-like factor
ztf-27	T09F3.1	Predicted zinc-finger transcription factor
taf-1	W04A8.7	TBP-associated factor
taf-5	F30F8.8	TBP-associated factor
ntl-2	B0286.4	Subunit of the CCR4/NOT-like transcription complex
mdt-6	Y57E12AL.5	Med6 family transcriptional mediator
crh-2	C27D6.4	cAMP response-element binding (CREB) homolog bZIP transcription factor
cbp-1 *	R10E11.1	CBP/p300 transcriptional coactivator homolog
let-607 *	F57B10.1	cAMP response-element binding protein H (CREBH) homolog bZIP transcription factor
Migration and adhesion related		
mig-10	F10E9.6	RIAM, lamellopodin, and Grb7 homolog
arr-1 *	F53H8.2	β-arrestin ortholog
kin-2	R07E4.6	Predicted regulatory subunit of a cAMP-dependent protein kinase
dgn-1	T21B6.1	Dystroglycan homolog
sdn-1	F57C7.3	Syndecan-2 homolog
unc-112 *	C47E8.7	Kindlin ortholog
pat-4	C29F9.7	Integrin-linked kinase ortholog
pat-6	T21D12.4	α-parvin ortholog
unc-97 *	F14D12.2	PINCH family protein
atn-1	W04D2.1	α-actinin homolog
unc-89	C09D1.1	Obscurin ortholog
mel-11	C06C3.1	Smooth muscle myosin-associated phosphatase regulatory subunit homolog
let-502	C10H11.9	Rho-associated protein kinase homolog
yap-1	F13E6.4	Yes-associated protein homolog
dyn-1	C02C6.1	Dynamin GTPase ortholog
fln-1	Y66H1B.2	Human filamin A ortholog
fln-2	C23F12.1	Filamin ortholog
deb-1	ZC477.9	Vinculin ortholog
mig-38 *	F40F11.2	Integrin-related
src-1 *	Y92H12A.1	Non-receptor tyrosine kinase c-src homolog
tln-1 *	Y71G12B.11	talin homolog
nmy-2 *	F20G4.3	Non-muscle myosin II heavy chain homolog
mlc-5 *	T12D8.6	Myosin II essential light chain ortholog
unc-112 *	C47E8.7	Kindlin ortholog
unc-97 *	F14D12.2	PINCH family protein

Gene name	Sequence	Protein description
nck-1	ZK470.5	Nck adaptor protein ortholog
mig-15	ZC504.4	Nck-interacting kinase ortholog
pxl-1	C28H8.6	Paxillin homolog
mlc-4	C56G7.1	Non muscle myosin II regulatory light chain homolog
ina-1 *	F54G8.3	α-integrin subunit
pat-2 *	F54F2.1	α-integrin subunit
pat-3	ZK1058.2	β-integrin subunit
vab-3 *	F14F3.1	Pax-6 transcription factor orthologue

[a] Using the JK4143 strain, DTC-specific RNAi knockdown of these genes was performed and gonad morphology was analyzed for turning defects.

* Asterisks indicate that reporter strains for the gene were also screened.

TABLE 2

DTC Expression of GFP or RFP With RNAi Treatment

	Percentage of DTCs with GFP or RFP expression			
Transgenic strains	**Control**	***cbp-1* RNAi**	***let-607* RNAi**	***tln-1* RNAi**
src-1p	87.6% (n=49)	18.5% (n=27)	23.1% (n=26)	n/a
tln-1p	92.5% (n=53)	0.0% (n=20)	4.4% (n=23)	52.9% (n=17)
nmy-2p	71.0% (n=107)	39.5% (n=86)	68.1% (n=94)	75.0% (n=60)
NMY-2	100% (n=37)	76.2% (n=21)	100% (n=8)	92% (n=25)
mig-38p	92.5% (n=80)	98.1% (n=54)	95.1% (n=82)	93.1% (n=58)
mig-24p	98.8% (n=81)	100% (n=95)	99.1% (n=106)	100% (n=10)
ppn-1p	99.1% (n=117)	96.0% (n=99)	98.0% (n=99)	100% (n=81)
let-607p	93.5% (n=93)	94.7% (n=75)	90.9% (n=22)	97.3% (n=37)
UNC-112	97.1% (n=70)	1.3% (n=75)	86.4% (n=66)	96.2% (n=52)
unc-97p	43.1% (n=58)	0.0% (n=24)	0.0% (n=27)	42.9% (n=35)
vab-3p	100% (n=28)	0.0% (n=32)	11.4% (n=44)	n/a
pat-2p	97.9% (n=48)	4.2% (n=48)	10.3% (n=78)	100% (n=22)
PAT-2	94.1% (n=67)	0.0% (n=42)	0.0% (n=39)	39.5% (n=43)
ina-1p	95.8% (n=144)	91.7% (n=96)	91.6% (n=143)	100% (n=84)
INA-1	100% (n=72)	98.5% (n=67)	96.9% (n=64)	100% (n=63)
PAT-3	100% (n=35)	100% (n=45)	96.9% (n=32)	100% (n=20)